Inorganic Chemistry

ARTICLE

pubs.acs.org/IC

Trivalent Actinide and Lanthanide Separations by Tetradentate Nitrogen Ligands: A Quantum Chemistry Study

Jian-Hui Lan,[†] Wei-Qun Shi,[†,*] Li-Yong Yuan,[†] Yu-Liang Zhao,[†] Jun Li,[‡] and Zhi-Fang Chai[†]

[†]Nuclear Energy Nano-Chemistry Group, Key Laboratory of Nuclear Analytical Techniques and Key Laboratory For Biomedical Effects of Nanomaterials and Nanosafety, Institute of High Energy Physics, Chinese Academy of Sciences, Beijing 100049, China

[‡]Department of Chemistry and Key Laboratory of Organic Optoelectronics and Molecular Engineering of Ministry of Education, Tsinghua University, Beijing 100084, China

Supporting Information

ABSTRACT: Although a variety of tetradentate ligands, 6,6′-bis(5,6-dialkyl-1,2,4-triazin-3-yl)-2,2′-bipyridines (BTBPs), have been proved as effective ligands for selective extraction of Am(III) over Eu(III) experimentally, the origin of their selectivity is still an open question. To elucidate this question, the geometric and electronic structures of the actinide and lanthanide complexes with the BTBPs have been investigated systematically by using relativistic quantum chemistry calculations. We show herein that in 1:1 (metal:ligand) type complexes substitution of electron-donating groups to the BTBP molecule can enhance its coordination ability and thus the energetic stability of the formed Am(III) and Eu(III) complexes in the gas phase. According to our results, Eu(III) can coordinate to the BTBPs with higher stability in energy than Am(III), no matter whether there are nitrate ions in the inner-sphere complexes. The presence of nitrate ions leads to formation of the probable Am(III) and Eu(III) complexes, $M(NO_3)_3(H_2O)_n$ (M = Am, Eu), in nitric acid solutions. It has been found that the changes of Gibbs free energy play an important role for Am(III)/Eu(III) separation. In fact, the weaker complexing ability of Am(III) with nitrate ions and water molecules makes the decomposition of $Am(NO_3)_3(H_2O)_4$ more favorable in energy, which may thus increase the possibility of formation of $Am(BTBPs)(NO_3)_3$. Our work may shed light on the design of novel extractants for Am(III)/Eu(III) separation.

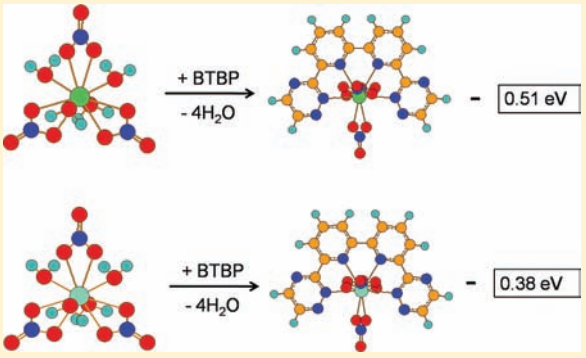

1. INTRODUCTION

Separation of trivalent actinides (An(III)) from lanthanides (Ln(III)) by solvent extraction is an important procedure for spent nuclear fuel reprocessing. In this procedure, one of the most challenging goals is to design efficient organic ligands (L) with high selectivity toward An(III). A series of theoretical investigations[1−12] has been performed to explore the complexation mechanisms[13−16] between ligands and heavy metal (M) ions, such as the donor−acceptor interaction, the charge transfer mechanism, the intrinsic relationship between geometry and electron structures, and the thermodynamic stability. These efforts can improve the design of novel ligands at the molecular level.

An(III) and Ln(III) show similar chemical properties in aqueous solution such as similar ion radii and conformations of hydrated ions. These features make An(III)/Ln(III) separation very troublesome industrially. In experiments, the separation process is generally determined by numerous factors such as coordinating ions, ionic strength, pH, kinetics of complexation, equilibration constants, number of coordinated water molecules, nature of substituent groups, cocktail of solvents, etc. The separation efficiency is determined by the synergy effects from these factors. Therefore, it is important to understand the role of these factors and their interaction mechanism. The rapid development of computational actinide chemistry has enabled us to probe the complexation between An(III), Ln(III), and ligands at the molecular level in the recent decades.[1−11] One viewpoint proposed by Nash and shared by others is that the selectivity of N- or S-donor ligands to An(III) over Ln(III) may originate from the slightly greater covalent character in An−L bonds, and the covalency difference may be the determining factor in the An(III)/Ln(III) separation process.[17] However, Cao et al. found that the Am(III)−S bonds are longer than Eu(III)−S bonds in Cyanex301 complexes, which is inconsistent with the general expectation that S- or N-donor ligands coordinate to An(III) with shorter M−L bonds than Ln(III) due to higher covalency in An−L bonds.[11] To date, it remains to be a challenging task to make clear the origin of the ligand selectivity, which requires development of novel theoretical methods and high-level experimental techniques.

To date, several families of N-donor ligands have been developed to extract An(III), such as tridentate Terpy, 2,4,6-tri(2-pyridyl)-1,3,5-triazine (Tptz), 2-amino-4,6-di(pyridin-2-yl)-1,3,5-triazine (Adptz), and 2,6-di(1,2,4-triazin-3-yl)pyridine (BTP), as well as

Received: January 13, 2011
Published: August 25, 2011

Scheme 1. BTBP Family of Molecules in ccc (cis, cis, cis) Conformation, where R Terminals Denote Substituents[a]

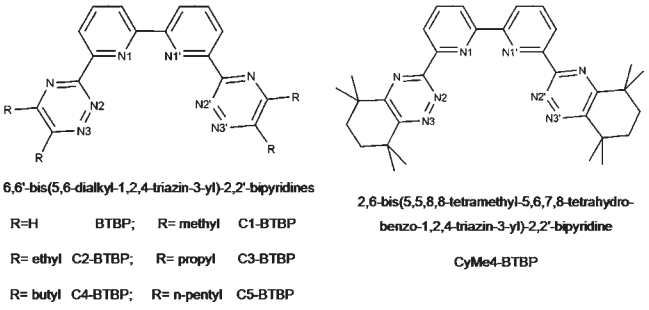

[a] NX and NX′ (X = 1−3) are equivalent approximately owing to rough C_2 symmetry.

their derivatives.[18−23] Among these ligands, the BTP family has been reported to display a high Am(III)/Eu(III) separation factor ($SF_{Am/Eu}$ = 130) in nitric acid systems.[24,25] However, the BTPs also have several drawbacks, like low stabilities with respect to acidic hydrolysis and radiolysis.[26,27] Recently, a new family of ligands, 6,6′-bis(5,6-dialkyl-1,2,4-triazin-3-yl)-2,2′-bipyridines (BTBPs),[28−37] was developed. As shown in Scheme 1, the BTBPs are hydrophobic, tetradentate nitrogen heterocyclic reagents and their side terminals can be substituted by others groups. The BTBP family has been found to be promising for extracting pentavalent and trivalent elements from tetravalent and hexavalent elements.[31] In addition, CyMe4-BTBP possesses not only high An(III)/Ln(III) separation efficiency but also excellent stability toward nitric acid.[29] Though abundant extraction experiments have been performed so far, there are still many unclear scientific issues in An(III) and Ln(III) coordination process with BTBPs, such as the origin of selectivity and the corresponding thermodynamics and kinetics. Compared to numerous BTBPs crystals concerning Ln(III),[28] there seems to be no reported crystals formed by An(III)−BTBPs complexes due to the strong radioactivity. This makes computational investigations more important for explaining An(III) complex behavior. Recently, Wipff et al. studied the basicity, complexation ability, and interfacial behavior of BTBPs using quantum chemistry and molecular dynamics simulations and reported that Eu(III) may be extracted via the protonated ligand form in acidic conditions.[12]

In this work, relativistic quantum chemical calculations were performed to explore the following issues: (i) the bonding nature of the BTBPs with An(III) and Ln(III); (ii) the impact of substituents on the geometry, electronic structure, and complexation strength of the BTBPs complexes; (iii) the possible complexing reactions for An(III) and Ln(III) with the BTBPs in nitric acid solutions. Here, Am(III) and Eu(III) were selected as representatives of actinides and lanthanides, respectively. A series of substituents, including alkyl groups from methyl to *n*-pentyl, methoxyl, and cyano, were considered. In addition, CyMe4-BTBP was also studied. These theoretical studies could provide insight into the complexation of An(III) and Ln(III) with tetradentate nitrogen-donor ligands and help the molecular design of selective ligands for An(III) extraction.

2. COMPUTATIONAL DETAILS

All quantum chemistry calculations were performed with the Gaussian 03 program.[38] Relativistic effects were considered with the quasi-relativistic effective core potentials (RECP) developed by the Stuttgart and Dresden groups together with the accompanying basis sets.[39−41] The adopted small-core RECPs replace 60 core electrons for actinides and 28 electrons for lanthanides, and the corresponding valence basis sets use a segmented contraction scheme for both of them. The spin−orbit coupling effects were not taken into consideration. For geometry optimization, the hybrid B3LYP method[42] was used, in combination with 6-31G(d) basis set for all other atoms. As reported by Guillaumont,[7] the increase of basis set size from 6-31G(d) to 6-311G(2d, p) at the DFT (B3LYP) level leads to a decrease of the M−L bond length by about 0.01 Å, and the MP2 and DFT methods give the bond length difference < 0.02 Å for An− and Ln−BTP complexes.

The targeted ligands and their complexes with Am(III) and Eu(III) were fully optimized without constraint. On the basis of the optimized structures, the binding energies were obtained by single-point energy calculations, including correction of thermal free energy at 298.15 K in the gas phase. Single-point energy calculations were carried out at the B3LYP level with the 6-311G(d, p) basis set for all light atoms. For metals, the same theoretical methods as those for geometry optimization were adopted. Natural population analysis (NPA) [13,43−46] was done on the optimized systems because it is less basis sets dependent.[43]

In this work, complexes with a 1:1 metal to ligand ratio were considered based on the observation that Am(III) and Eu(III) can form 1:1 and 1:2 complexes with BTBPs in experiments. [26−29,31,46−48] Given the large computational cost, we first adopted a simple theoretical model $[ML]^{3+}$ to explore the influence of substituents on the complexation ability of ligands and the M−L bonding nature in the complexes. In aqueous solution, the counterions and solvents may influence formation of complexes significantly, especially the structural parameters. Therefore, we then adopted the more common complex $ML(NO_3)_3$ to investigate the influence of counterions and solvents. The possible complexing reactions for Am(III) and Eu(III) with BTBPs in nitric acid solutions were studied, and the thermodynamic properties were discussed in detail.

3. RESULTS AND DISCUSSION

Both experimental and theoretical investigations show that the BTBPs possess six possible conformations in the gas phase and solution.[28] Among these conformations, the ccc in Scheme 1 is considered as the most favorable one during the chelating process. Our calculations show that the BTBPs and their complexes with Am(III) and Eu(III) display C_2 symmetry roughly. Therefore, N1 and N1′, N2 and N2′, as well as N3 and N3′ are approximately equivalent in Scheme 1. Subsequently, the geometry properties, charge distributions, and bonding natures in M−L (M = Am or Eu, L = BTBPs) complexes will be analyzed in detail to provide insight into An(III) extraction.

3.1. $[ML]^{3+}$ Complexes. To explore the impact of substituents on the complexation ability of ligands, the $[AmL]^{3+}$ and $[EuL]^{3+}$ complexes are first investigated in this section, where L denotes the BTBPs. In this work, the small-core ECPs were adopted to treat the f shell explicitly. We expect that treatment of the f shell as the valence shell can give reliable predictions of chemical properties for actinides and lanthanides. To test the reliability of our theoretical methods, we selected the trifluoride europium (EuF_3) as a theoretical model and optimized it at the DFT, Hartree−Fock (HF), and configuration interaction (CISD) levels in combination with the same ECPs and basis sets. On the basis of our calculations, these theoretical methods give comparable predictions on the Eu−F bond which are close to the experimental values.[44,45] We can see from Table 1 that most of the predicted values (2.04 Å) are within a reasonable range except for the one (2.05 Å) by the HF method. Therefore, it is

dx.doi.org/10.1021/ic200078j |*Inorg. Chem.* 2011, 50, 9230–9237

Table 1. Equilibrium Bond Distances in EuF_3 Calculated at the DFT, HF, and CISD Levels in Combination with Small-Core RECPs

	B3LYP	PBE	PW91	HF	CISD	exp.[a]
D_{Eu-F}	2.04	2.04	2.04	2.05	2.04	2.02

[a] The estimated uncertainty is ±0.02Å

Table 2. Calculated Interaction Distances from Central Metal Ions to Neighboring Nitrogen Atoms in $[AmL]^{3+}$ and $[EuL]^{3+}$ Complexes (L = BTBPs)

		bond lengths (Å) in $[ML]^{3+}$ complexes[a,b]								
		BTBP	C1-	C2-	C3-	C4-	C5-	CyMe4-	MO-	CN-
M−N1	Am	2.54	2.55	2.55	2.55	2.56	2.56	2.56	2.54	2.53
	Eu	2.54	2.54	2.55	2.55	2.55	2.55	2.55	2.53	2.55
M−N2	Am	2.37	2.35	2.35	2.34	2.34	2.34	2.34	2.33	2.38
	Eu	2.45	2.44	2.44	2.44	2.44	2.47	2.46	2.45	2.48

[a] In this table ligands are represented with their substituents. [b] Only a part of the bond distances are listed owing to rough C_2 symmetry of complexes.

believed that the adopted methods in this work can predict the geometric structures of the studied complexes reasonably.

Geometry. Complexes of $[AmL]^{3+}$ and $[EuL]^{3+}$ (L = BTBPs) were then studied based on the above work. Table 2 lists the calculated bond distances between the central metal ions and the coordinated nitrogen atoms in the studied complexes. The optimized structures of Am(III) and Eu(III) complexes are displayed in Figure S1 in the Supporting Information. In Table 2, the calculated Am−N1 bond is close to the Eu−N1 bond in length in the studied complexes with differences of no more than 0.02 Å, while the Am−N2 bond is obviously shorter than the Eu−N2 bond. In $[Am(BTBP)]^{3+}$, the Am−N2 bond is about 2.37 Å, which is much shorter than 2.45 Å for the Eu−N2 bond in the $[Eu(BTBP)]^{3+}$ complex. Taking into account the difference of ion radii (r_{Am} = 0.98 Å; r_{Eu} = 0.95 Å),[46] the Am−N2 bond is about 0.11 Å shorter than the Eu−N2 bond. These results may indicate the higher covalency in the Am−N2 bond compared with the Eu−N2 bond when no counterion or water exists in the inner-sphere complexes. As the alkyl substituents extend in length, the M−N2 bond displays a tendency to decrease. However, the $[Am(CN\text{-}BTBP)]^{3+}$ complex possesses the longest Am−N2 bond (2.38 Å) and the shortest Am−N1 bond (2.53 Å). The above changes can be attributed to the electron-donating and -withdrawing abilities of the studied substituents as discussed below. In contrast, the Eu−N2 bond distance shows a much slighter tendency to decrease. Furthermore, the Eu−N2 bond in $[Eu(CN\text{-}BTBP)]^{3+}$ reaches 2.48 Å and is still the longest among the studied complexes. It can also be deduced that the BTBPs mainly coordinate with metal ions via N2 and its counterpart N2′ in $[ML]^{3+}$ complexes.

Electronic Structures. The charge distribution, especially the atomic charges on nitrogen, may be an important factor that impacts the ligand chelating ability. Table 3 lists the calculated orbital population occupancy and spin densities of the f shell as well as a part of the NPA charges in the studied complexes. The remaining NPA data are displayed in Table S1, Supporting Information. For simplification, the net charges of central pyridine rings and lateral rings including substituents are denoted as Q_c and Q_l while the atomic charges on N1, N2, and N3 are described as q_{N1}, q_{N2}, and q_{N3}, respectively. According to our calculations, the studied alkyl and methoxyl groups produce comparable electron-donating effects but the cyano group shows strong electron-withdrawing ability, respectively. We also found that the changes of electron density on the coordinated nitrogen follow a similar trend to those on the central pyridine rings after substitution, as displayed in Figure 1.

After complexing with Am(III) and Eu(III), we observed that there is a charge flow from the BTBPs to the metal ions, leading to a significant charge decrease of the central metal ions (<3). This phenomenon indicates a significant electron donor−acceptor interaction in the formed complexes. Actually, this interaction may predominantly originate from the induced polarization of ligands by the chelated cations. The changes of atomic charge on Am and Eu ions (Δq) remain as $0.549\ e \leq \Delta q \leq 0.881\ e$ ($e = 1.6 \times 10^{-19}$ C), suggesting that there may exist covalent character in M−L bonding (M = Am or Eu, L = BTBPs). It should be mentioned that the coordinated Am ions show more positive charges than Eu ions in the studied complexes, for example, q_{Am} = 2.433 e in $[Am(BTBP)]^{3+}$ and q_{Eu} = 2.232 e in $[Eu(BTBP)]^{3+}$. The stronger electron affinity of Eu(III) may result from the so-called lanthanide contraction and the weaker nucleus-screening ability of the 4f shell. Therefore, the ionic interaction in Am−N bonds seems to be stronger than that in Eu−N bonds, because of the larger absolute charge values on N and Am ions in $[ML]^{3+}$ complexes. As listed in Table S1, Supporting Information, there exists a relationship of $Q_c < Q_l$ for most Am and Eu complexes, indicating that the electron-donor groups make the lateral rings lose more electrons during the coordination process.

As shown in Figure 1, as the terminal alkyl group extends from methyl to *n*-pentyl, the positive charges on the Am ion decrease gradually whereas the negative charges on N1, N2, and N3 decrease. The increase of electron density might stem from the electron transfer from the lateral rings as well as the substituted alkyl groups to the Am center, which indicates enhancement of donor−acceptor interaction in Am complexes. By comparison, we see that the methoxyl group shows comparable electron-donating abilities with *n*-pentyl. In contrast, the presence of cyano groups leads to a significant decrease of electron densities on the Am ion, central pyridine rings, and coordinated nitrogen atoms. For $[EuL]^{3+}$ (L = BTBPs) complexes, similar trends are observed. On the basis of Mulliken population, the f levels in the complexes are occupied by additional electrons compared with free trivalent cations. In addition, the Eu ion has slightly higher f-occupancy numbers than the Am ion, proving its stronger electron affinity again. The f spins of the Am ion are also found to be lower than those of the Eu ion. For the test system EuF_3, the f occupancy and spin density reach 6.08 and 5.97, respectively, that is, about three valence electrons of Eu are donated to F atoms in EuF_3

To explore the M−L bonding nature, the bond overlap population (OP) in the studied complexes was also performed. The OP in chemical bonds is widely considered as the degree of covalency. In the BTBPs complexes, the overlap values in a covalent single bond such as C−H bond are within the range of 0.8−0.9. In the covalent C−C bond of the heterocyclic rings, the overlap values are between 1 and 1.5 due to formation of a conjugated π bond. However, the very small overlap values in M−L bonds indicate that the ionic interaction is predominant for Am(III) and Eu(III) complexes. As shown in Table 4, the M−N2

dx.doi.org/10.1021/ic200078j |*Inorg. Chem.* 2011, 50, 9230–9237

Table 3. Calculated Mulliken Orbital Occupancy, Spin Density of f Shells, and NPA Charge Distribution in $[ML]^{3+}$ (M =Am, Eu; L = BTBPs)[a]

			charges in $[ML]^{3+c}$			
ligand[b]	f occupancy	f spin	q_{N1}	q_{N2}	q_{N3}	q_M
C0-	6.40/6.62	6.15/6.54	−0.659/−0.645	−0.494/−0.447	−0.209/−0.158	2.433/2.232
C1-	6.41/6.64	6.13/6.56	−0.654/−0.642	−0.506/−0.460	−0.244/−0.189	2.410/2.208
C2-	6.43/6.67	6.16/6.59	−0.652/−0.696	−0.507/−0.476	−0.254/−0.176	2.399/2.160
C3-	6.43/6.67	6.16/6.59	−0.651/−0.639	−0.511/−0.464	−0.253/−0.195	2.395/2.181
C4-	6.43/6.69	6.16/6.61	−0.650/−0.638	−0.513/−0.466	−0.256/−0.199	2.392/2.167
C5-	6.43/6.74	6.17/6.67	−0.649/−0.635	−0.514/−0.471	−0.257/−0.211	2.389/2.119
CyMe4-	6.44/6.73	6.18/6.66	−0.650/−0.636	−0.513/−0.456	−0.256/−0.185	2.392/2.130
MO-	6.41/6.68	6.13/6.61	−0.653/−0.314	−0.544/−0.496	−0.365/−0.637	2.417/2.167
CN-	6.38/6.66	6.13/6.59	−0.662/−0.635	−0.492/−0.452	−0.180/−0.146	2.451/2.200

[a] Atomic unit of e is used for charge and ..../... refers to the results for $[AmL]^{3+}$ and $[EuL]^{3+}$, respectively. [b] All ligands are represented by their substituents, and C0 denotes the nonsubstituted BTBP. [c] q_{N1}, q_{N2}, q_{N3}, and q_M denote charges on N1, N2, N3, and central metal ion, respectively.

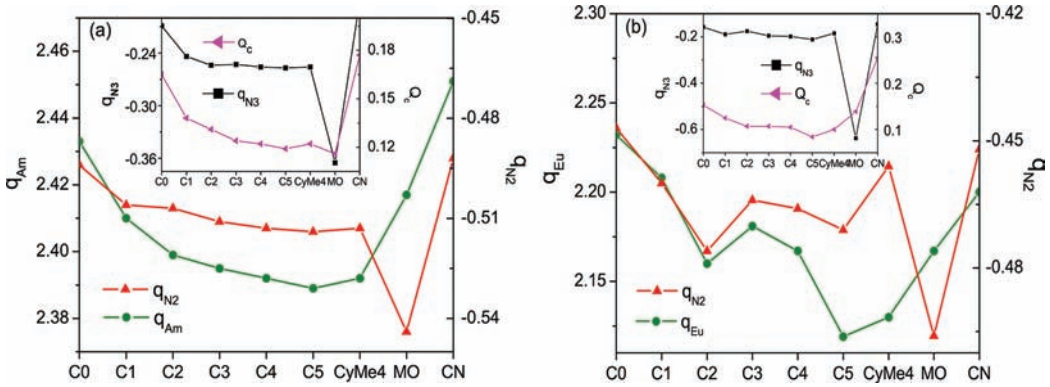

Figure 1. NPA charges on the central pyridine rings (Q_c), the nitrogen atoms (q_{N2} and q_{N3}), and the metal ions (q_{Am} and q_{Eu}) in (a) $[AmL]^{3+}$ and (b) $[EuL]^{3+}$ complexes as a function of ligands (L = BTBPs). The BTBPs are represented by their substituents and C0- denotes the nonsubstituted BTBP for simplicity.

Table 4. Calculated Bond Overlap Populations in Complexes of $[AmL]^{3+}$ and $[EuL]^{3+}$ (L = BTBPs)

		bond overlap populations in $[ML]^{3+}$ complexes[a]								
		C0-	C1-	C2-	C3-	C4-	C5-	CyMe4-	MO-	CN-
N1	Am	0.148	0.143	0.141	0.140	0.139	0.139	0.139	0.142	0.152
	Eu	0.102	0.099	0.108	0.095	0.093	0.088	0.091	0.091	0.093
N2	Am	0.210	0.223	0.224	0.227	0.229	0.229	0.229	0.236	0.205
	Eu	0.122	0.123	0.116	0.118	0.112	0.088	0.102	0.114	0.099

[a] BTBPs are represented by substituents, and C0- denotes the nonsubstituted BTBP. Only the OPs of several M−L bonds are listed owing to rough C_2 symmetry.

bonds show larger overlap values than M−N1 bonds, which may indicate their higher covalency, while the substituents just show a slight impact on the OPs. We also found that the OPs and M−N2 bond lengths show similar trends as the substituents change. Most substituents reduce the OPs in both Eu−N1 and Eu−N2 bonds in Eu(III) complexes with BTBPs, making the Eu−N bond more ionic. Cao et al. found that the An(III)−S bonds are longer than Eu(III)−S bonds in Cyanex301 complexes,[11] which might indicate the absence of the expected covalency in An(III)−S bonds. They proposed that the hydration Gibbs free energies for M^{3+} may play an important role for the high selectivity of Cyanex301 toward Am(III) and Cm(III) over Eu(III). However, considering the difficulty in accurate evaluation of covalency, development of modern chemical bond theory and advanced experimental techniques are needed to make clear the M−L bonding nature.

Generally, the relatively diffuse 5f orbitals might participate in the chemical bonding of these complexes, and the energy levels with predominant 5f character exist in the frontier orbitals. Figure 2 presents the calculated main energy level mixing between metal and ligand moieties in $[Am(CyMe4\text{-}BTBP)]^{3+}$ and $[Eu(CyMe4\text{-}BTBP)]^{3+}$ complexes. Here, we just consider the level mixing relevant to the lone pars of N2 and its counterpart. According to our calculations, the top two highest occupied molecular orbitals (HOMO) of the ligand moiety are occupied by the lone pairs of N2 and N2′, forming two nearly degenerate levels. In addition, the lowest unoccupied molecular orbital (LUMO) of the ligand is assigned as a π^* orbital, being formed by the overlap of conjugated C and N $2p_z$ orbitals in the heterocycles. As for Am or Eu moieties, the $(n-2)$f subshell become the HOMO. Furthermore, the *ns* levels rise significantly after losing two electrons. In Figure 2, the energy level difference $\Delta(5f \rightarrow n(lp))$ in Am(III) complex is smaller by about 3.49 eV

dx.doi.org/10.1021/ic200078j |*Inorg. Chem.* 2011, 50, 9230–9237

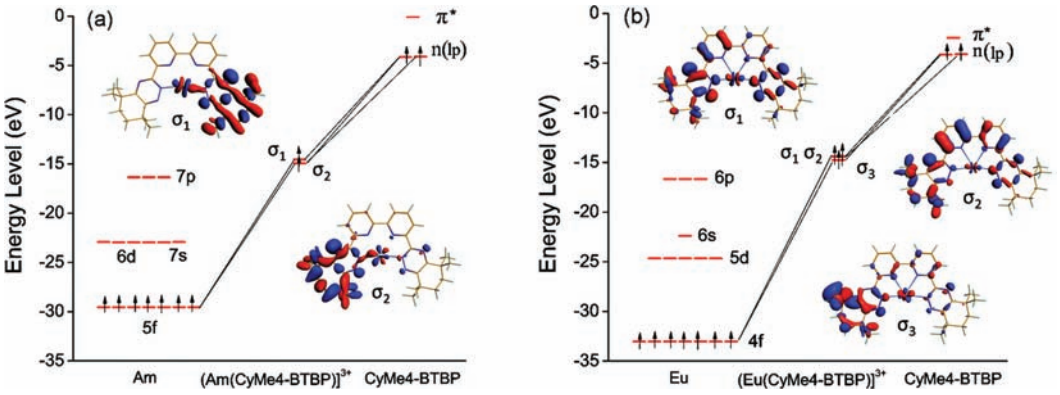

Figure 2. Main energy level mixing between metal and ligand moieties in (a) $[Am(CyMe4\text{-}BTBP)]^{3+}$ and (b) $[Eu(CyMe4\text{-}BTBP)]^{3+}$ complexes. Only orbitals with alpha-spin state are listed. The f orbitals of Eu(III)/Am(III) are partially occupied, as listed in Table 3. The inset gives the M−L molecular orbital diagrams relevant to the lone pairs (lp) of N2 and N2′. The molecules are displayed in stick mode, and yellow, cyan, blue, green, and light blue represent C, H, N, Am, and Eu atoms, respectively. The isosurface value of the molecular orbitals is set to be 0.03 au.

Table 5. Calculated Binding Energies for the $[ML]^{3+}$ Complexes.

	ΔG (eV) for reaction of L + M^{3+} → $[ML]^{3+a}$								
	C0-	C1-	C2-	C3-	C4-	C5-	CyMe4-	MO-	CN-
Am	−19.43	−20.76	−21.11	−21.30	−21.68	−21.54	−21.39	−21.39	−17.29
Eu	−20.67	−21.79	−22.19	−22.39	−22.59	−23.03	−22.58	−22.38	−18.28

[a] BTBPs are represented by their substituents.

than $\Delta(4f \rightarrow n(lp))$ in the Eu(III) complex, leading to slightly stronger Am−N orbital overlaps. For Am(III) complex, the lone pairs of N2 and N2′ mainly participate in formation of two nearly degenerate bonding orbitals, σ_1 and σ_2. For the Eu complex, three nearly degenerate bonding orbitals, σ_1, σ_2, and σ_3, are formed. However, the M−L orbital interaction is obviously weaker in Eu complexes as shown in the insets, proving that the Eu−N bonds are less covalent than Am−N bonds. In addition, using the topological methodology of electron localization function (ELF),[47] the higher covalency in Am−N bonds can also be observed for $[ML]^{3+}$ (see the Supporting Information).

Thermodynamics. To explore the relationship between the covalency of M−L bonds and the stability of complexes, we also calculated the binding energy of the studied Am(III) and Eu(III) complexes (see Table 5). The binding energy is defined as

$$\Delta G = G([ML]^{3+}) - G(M^{3+}) - G(L) \quad (1)$$

where G is the electronic energy contribution with Gibbs free energy correction. According to our calculations, the Eu(III) complexes seem to be more stable in energy than the Am(III) complexes, though the Am−N bonds are more covalent. For both Am(III) and Eu(III) complexes, their energetic stability increases as the alkyl substituents extend, indicating that the substituents with stronger electron-donating ability can make the formed complexes more stable in energy. These results explain why the cyano-substituted complexes have the worst stability while the methoxyl-substituted complexes are more stable. It is surprising that the higher covalency in Am−N bonds does not make the Am(III) complexes more stable in energy, which might suggest the dominant role of ionic interaction in those complexes. In the next part, we will focus on the more common $ML(NO_3)_3$ complexes to explore the complexation mechanism of the BTBPs with Am(III) and Eu(III) in nitric acid solutions.

3.2. $ML(NO_3)_3$ Complexes. As is well known, coordination of counterions and solvents may have a non-negligible impact on formation of M−L complexes in aqueous solution. Here, we adopted BTBP and CyMe4-BTBP as representatives and then studied their possible complexation processes with Am(III) and Eu(III) as well as nitrate ions. In experiments, the $M(BTBPs)\text{-}(NO_3)_3$-type complexes are found to be favorable for Eu(III) in nitrate-rich solutions. Drew et al. reported that the majority of the structures show the lanthanide to be 10 coordinated with a stoichiometry $Ln(BTBPs)(NO_3)_3$.[28] Another work reported by Drew et al. proposed that the extracted Am(III) compound may appear in the form of $[Am(NO_3)_3(C2\text{-}BTBP)]$ experimentally.[36] On the basis of these investigations, we then studied the geometries and thermodynamic stabilities of the $Am(BTBPs)\text{-}(NO_3)_3$ and $Eu(BTBPs)(NO_3)_3$ species. Figure 3 gives the optimized structures of $AmL(NO_3)_3$ and $EuL(NO_3)_3$ complexes, where L denotes the nonsubstituted BTBP and CyMe4-BTBP. According to our calculations, three nitrate ions can coordinate to the Am and Eu centers at most in 1:1 complexes with one in the ligand plane (NO_3^-_i) and two out of the plane (NO_3^-_o). In these complexes, the nitrate ions are bidentate ligands when coordinating to the metal center, resulting in the metal coordination number of 10.

As listed in Table 6, coordination of nitrate ions makes the M−N bonds elongated by about 0.1−0.3 Å than those observed previously. In the presence of NO_3^-, the M−N2 bonds are still shorter than the M−N1 bonds. In addition, CyMe4-BTBP can bind Am(III) or Eu(III) with shorter M−N bonds than BTBP, owing to the strong electron-donating ability of the substituents. More importantly, the Am−N bonds are longer than the Eu−N bonds in both BTBP and CyMe4-BTBP complexes, which is different from observations in the absence of nitrate ions. Similar trends were also found in Cyanex301 complexes by Cao et al. recently, where Am−S bonds are found to be longer than Eu−S bonds.[11] The structural parameters of the inner-sphere nitrate ions are also listed in Table 6. In both BTBP and CyMe4-BTBP complexes, the average distances between the Am center and the coordinated oxygen atoms in out-of-plane nitrate ions (Am−O_o) are about 2.54 Å, which is about 0.03 Å longer than the average Eu−O_o distances. As for the Am(III) and Eu(III) complexes

dx.doi.org/10.1021/ic200078j |*Inorg. Chem.* 2011, 50, 9230–9237

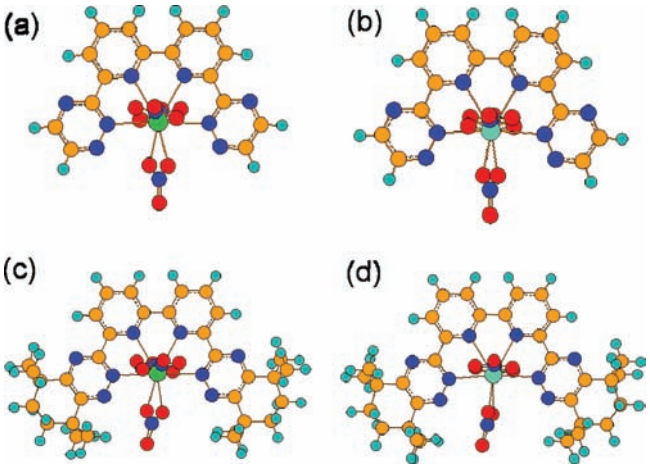

Figure 3. Optimized structures of $AmL(NO_3)_3$ and $EuL(NO_3)_3$ complexes, where L denotes the BTBPs: (a) $Am(BTBP)(NO_3)_3$, (b) $Eu(BTBP)(NO_3)_3$, (c) $Am(CyMe4\text{-}BTBP)(NO_3)_3$, and (d) $Eu(CyMe4\text{-}BTBP)(NO_3)_3$. Yellow, cyan, blue, red, green, and light blue spheres represent C, H, N, O, Am, and Eu atoms, respectively.

Table 6. Calculated Structural Parameters (Å) in $ML(NO_3)_3$ (M = Am, Eu; L = BTBPs) Complexes[a]

		N1	N2	O_o[b]	O_i[c]
C0-	Am	2.74	2.63	2.54	2.47
	Eu	2.70	2.60	2.51	2.43
CyMe4-	Am	2.73	2.60	2.54	2.49
	Eu	2.65	2.58	2.51	2.46

[a] Bond distances are averaged, and BTBPs are represented by substituents. [b] O_o denotes the coordinated oxygen in the out-of-plane nitrate ions. [c] O_i denotes the coordinated oxygen in the nitrate ions within the complex surface.

with the same ligand, the average Am−O_i bonds are also evidently longer than the Eu−O_i bonds.

The inner-sphere nitrate ions also influence the M−L bonding in the studied complexes. In Table 7, the bond overlap populations in Am−N and Eu−N bonds decrease significantly in the $ML(NO_3)_3$ complexes in comparison with those in $[ML]^{3+}$. The very subtle discrepancies of overlaps in Am−N and Eu−N bonds might suggest the similar M−L bonding nature in $ML(NO_3)_3$ complexes, that is, the slightly longer Am−N bonds than Eu−N bonds may originate from the ion radii differences between Am(III) and Eu(III). In terms of the obtained bond overlap populations, the An−N bonds seem to show comparable covalency with Ln−N bonds. Subsequently, we compared the thermodynamic stability of $ML(NO_3)_3$ complexes by defining the binding energy as

$$\Delta G = G(ML(NO_3)_3) - G(M^{3+}) - G(L) - 3G(NO_3^-) \quad (2)$$

For $Am(BTBP)(NO_3)_3$ and $Eu(BTBP)(NO_3)_3$, the calculated binding energies are about −44.17 and −44.75 eV, respectively. As for $Am(CyMe4\text{-}BTBP)(NO_3)_3$ and $Eu(CyMe4\text{-}BTBP)(NO_3)_3$, the obtained values are about −44.43 and −45.08 eV, respectively. Our results seem to suggest that formation of $Am(BTBPs)(NO_3)_3$ and $Eu(BTBPs)(NO_3)_3$ complexes in solution

Table 7. Calculated Bond Overlap Populations in $ML(NO_3)_3$ (M = Am, Eu; L = BTBPs) Complexes[a]

L	M	N1	N1′	N2	N2′
C0-	Am	0.018	0.018	0.023	0.001
	Eu	0.015	0.015	0.017	0.016
CyMe4-	Am	0.018	0.019	0.028	0.028
	Eu	0.066	0.064	0.063	0.061

[a] BTBPs are represented by their substituents.

is probable, which agrees well with experimental observations.[28,36] We can also see that Eu(III) has a slightly stronger complexation ability with the BTBPs than Am(III), which is independent of counterion or solvent coordination.

On the basis of the above results, we then focused on the changes of the thermodynamic properties during the Am(III)/Eu(III) separation process. In aqueous solution, the spherical Am(III) and Eu(III) ions prefer to form hydrated ions with the 8 to 9 coordination number,[48,49] and these coordinated water molecules can also be replaced by ligands with similar or stronger binding energies. In the presence of enough NO_3^-, the hydrated neutral nitrate complexes may be produced with several water molecules to fully occupy the inner-sphere space. Skarnemark et al. also suggested the complexing process of $Am^{3+} + 3NO_3^- \rightarrow Am(NO_3)_3(H_2O)_n$ in acid solution, where n is equal to the maximal 4−6.[31] According to our DFT calculations, in $M(NO_3)_3(H_2O)_n$ (M = Am or Eu) complexes, four water molecules can be coordinated to the metal center with a coordination number of 10 at most. Figure 4 displays the optimized structures of $M(NO_3)_3(H_2O)_n$ (M = Am, Eu; n = 2, 3, and 4) complexes. We see that the average M−L interaction distances are elongated gradually as the number of water molecules increases and the Gibbs free energies of the complexes decrease. In $Am(NO_3)_3(H_2O)_4$ complex, the average Am−O_{water} and Am−$O_{nitrate}$ distances are about 2.59 and 2.52 Å, respectively. In $Eu(NO_3)_3(H_2O)_4$ complex, the average Eu−O_{water} and Eu−$O_{nitrate}$ distances reach 2.56 and 2.48 Å, respectively. Given that the optimizations were performed in the gas phase, it can be deduced that the bond distances may be elongated to some extent, as observed for hydrated ions.[48,49] Though the neutral nitrate complex can be extracted to the organic phase, however, the presence of water in the inner sphere will decrease the solubility of complexes in organic solvents. Therefore, formation of neutral complex with a large and an essentially aromatic ligand will help to improve the efficiency of extraction into organic solvents.

On the basis of the favorable complexes of Am(III) and Eu(III) in nitric acid systems, Skarnemark et al. suggested the following complexing reaction $M(NO_3)_3 + BTBPs \rightarrow M(NO_3)_3(BTBPs)$, where the coordinated water is neglected.[30,31] In this work, we adopted one of the probable complexing processes at the interface between water and organic phase as representative

$$M(NO_3)_3(H_2O)_4 + L \rightarrow ML(NO_3)_3 + 4H_2O \ (L = BTBPs) \quad (3)$$

Our results show that in the presence of the BTBP molecule the changes of Gibbs free energy of reaction 3 for Am(III) and Eu(III) reach −0.54 and −0.41 eV, respectively. Because DFT methods are basically reliable in predicting the trends of chemical properties, we deduce that the complexing reaction for Am(III) is more preferable in

dx.doi.org/10.1021/ic200078j |Inorg. Chem. 2011, 50, 9230–9237

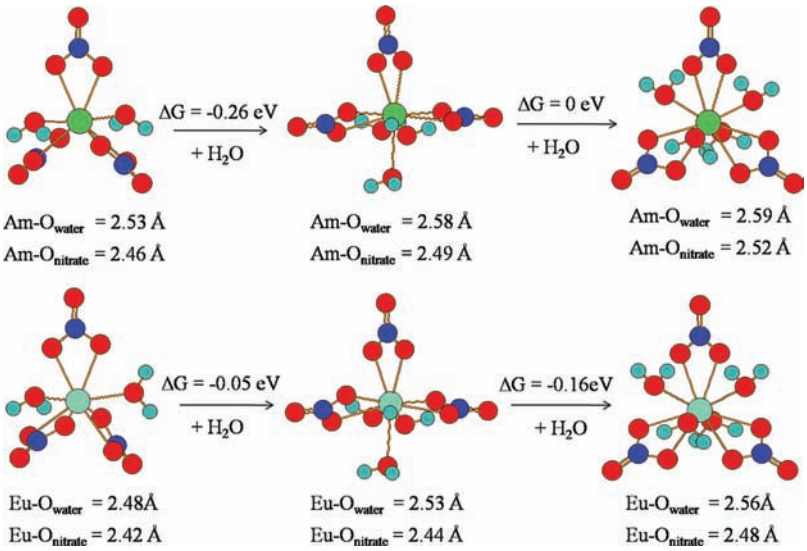

Figure 4. Probable complexes for Am(III) and Eu(III) with nitrate ions and water molecules in nitric acid solutions. Changes of gas-phase Gibbs free energy and average interaction distances are also presented. Cyan, blue, red, green, and light blue spheres represent H, N, O, Am, and Eu, respectively.

energy compared to that for Eu(III). In contrast, when CyMe4-BTBP is used, the calculated changes of Gibbs free energy are −0.80 and −0.73 eV for Am(III) and Eu(III), respectively. All complexing reactions are found to be exothermic according to our calculations. By comparison, we see that complexation of CyMe4-BTBP with Am(III) and Eu(III) is more favorable compared with that of BTBP. The preference toward formation of $Am(BTBPs)(NO_3)_3$ may result from the lower stability of $Am(NO_3)_3(H_2O)_4$ than $Eu(NO_3)_3(H_2O)_4$, which can make the former easier to decompose and thus increases the formation probability of $Am(BTBPs)(NO_3)_3$ complexes. These findings agree well with the experimental results.[28,30,31,36] Finally, the stronger complexation ability of Eu(III) with ligands including nitrate ions and water molecules may play an important role for Am(III)/Eu(III) separation.

4. CONCLUSIONS

The complexation mechanism of the BTBPs with Am(III) and Eu(III) was studied in this work by using relativistic DFT calculations. In terms of our calculations, the nitrogen atoms of N2 and N2′ in the lateral heterocyclic rings of the BTBPs may play a dominant role when coordinated to Am(III) and Eu(III). It has been found that substitution of electron-donor groups to the BTBP molecule can enhance its coordination ability in the gas phase and thus slightly strengthen the stability of the formed Am(III)−L and Eu(III)−L complexes in energy. In contrast, the electron-acceptor groups exert an opposite effect.

According to bond overlap populations, the M−N bonds in $M(BTBPs)(NO_3)_3$ (M = Am or Eu) have mainly ionic features. In addition, the Am(III) complexes are less stable compared to the Eu(III) complexes, no matter whether there are nitrate ions in the inner sphere. In nitric acid solutions, Am(III) and Eu(III) can complex with nitrate ions and water molecules and the 10-coordinated $M(NO_3)_3(H_2O)_4$ complexes are found to be favorable for both of them based on our calculations. The related experimental and our DFT studies indicate that the complexation reaction $M(NO_3)_3(H_2O)_4 + L \rightarrow ML(NO_3)_3 + 4H_2O$ (M = Am or Eu; L = BTBPs) is probable at the interface between water and the organic phase. In this reaction, formation of $Am(BTBPs)(NO_3)_3$ is found to be more favorable than $Eu(BTBPs)(NO_3)_3$ energetically, which may result from the weaker complexing ability of Am(III) with nitrate ions and water, that is, formation of $M(BTBPs)(NO_3)_3$ may depend on the decomposition of $M(NO_3)_3(H_2O)_4$ strongly for Am(III) and Eu(III). In summary, the changes of Gibbs free energy play an important role for Am(III)/Eu(III) separation. We expect that this work can provide useful information for designing novel extractants for Am(III)/Eu(III) separation, and in the future, we will further investigate the complexation mechanism of 1:2-type BTBP complexes.

■ ASSOCIATED CONTENT

Supporting Information. Additional information concerning the optimized structures, ELF topology analysis, charge distribution of $[ML]^{3+}$ complexes. This material is available free of charge via the Internet at http://pubs.acs.org.

■ AUTHOR INFORMATION

Corresponding Author
*E-mail: shiwq@ihep.ac.cn

■ ACKNOWLEDGMENT

This work was supported by the National Natural Science Foundation of China (Grant Nos. 91026007 and 91026003) and the "Strategic Priority Research Program" of the Chinese Academy of Sciences (Grant Nos. XDA03010401 and XDA03010403). The results described in this work are obtained on the ScGrid of Supercomputing Center, Computer Network Information Center of Chinese Academy of Sciences.

■ REFERENCES

(1) Coupez, B.; Boehme, C.; Wipff, G. *Phys. Chem. Chem. Phys.* **2002**, *4*, 5716.
(2) Schurhammer, R.; Erhart, V.; Troxler, L.; Wipff, G. *J. Chem. Soc., Perkin Trans. 2* **1999**, 2423.
(3) Berny, F.; Muzet, N.; Troxler, L.; Dedieu, A.; Wipff, G. *Inorg. Chem.* **1999**, *38*, 1244.

(4) Chatterjee, T.; Sarma, M.; Das, S. K. *Cryst. Growth Des.* **2010**, *10*, 3149.
(5) Meskaldji, S.; Belkhiri, L.; Arliguie, T.; Fourmigue, M.; Ephritikhine, M.; Boucekkine, A. *Inorg. Chem.* **2010**, *49*, 3192.
(6) Ionova, G.; Rabbe, C.; Guillaumont, R.; Ionov, S.; Madic, C.; Krupa, J. C.; Guillaneux, D. *New J. Chem.* **2002**, *26*, 234.
(7) Guillaumont, D. *J. Phys. Chem. A* **2004**, *108*, 6893.
(8) Petit, L.; Adamo, C.; Maldivi, P. *Inorg. Chem.* **2006**, *45*, 8517.
(9) Petit, L.; Joubert, L.; Maldivi, P.; Adamo, C. *J. Am. Chem. Soc.* **2006**, *128*, 2190.
(10) Maldivi, P.; Petit, L.; Adamo, C.; Vetere, V. *C. R. Chimie* **2007**, *10*, 888.
(11) Cao, X.; Heidelberg, D.; Ciupka, J.; Dolg, M. *Inorg. Chem.* **2010**, *49*, 10307.
(12) Benay, G.; Schurhammer, R.; Wipff, G. *Phys. Chem. Chem. Phys.* **2011**, *13*, 2922.
(13) Reed, A.; Curtiss, L. A.; Weinhold, F. *Chem. Rev.* **1988**, *88*, 899.
(14) Gutman, V. *The Donor-Acceptor Approach to Molecular Interactions*; Plenum Press: New York, 1980.
(15) Hancock, R. D.; Martell, A. E. *Chem. Rev.* **1989**, *89*, 1875.
(16) Hancock, R. D.; Martell, A. E. *Adv. Inorg. Chem.* **1995**, *42*, 89.
(17) Nash, K. L. *Solvent Extr. Ion Exch.* **1993**, *11*, 729.
(18) Boubals, N.; Drew, M. G. B.; Hill, C.; Hudson, M. J.; Iveson, P. B.; Madic, C.; Russell, M. L.; Youngs, T. G. A. *Dalton Trans* **2001**, 55.
(19) Drew, M. G. B.; Guillaneux, D.; Hudson, M. J.; Iveson, P. B.; Russell, M. L.; Madic, C. *Inorg. Chem. Commun.* **2001**, *4*, 12.
(20) Drew, M. G. B.; Guillaneux, D.; Hudson, M. J.; Iveson, P. B.; Madic, C. *Inorg. Chem. Commun.* **2001**, *4*, 462.
(21) Boucher, C.; Drew, M. G. B.; Giddings, P.; Harwood, L. M.; Hudson, M. J.; Iveson, P. B.; Madic, C. *Inorg. Chem. Commun.* **2002**, *5*, 596.
(22) Drew, M. G. B.; Hill, C.; Hudson, M. J.; Iveson, P. B.; Madic, C.; Youngs, T. G. A. *Dalton Trans.* **2004**, 244.
(23) Denecke, M. A.; Rossberg, A.; Panak, P. J.; Weigl, M.; Schimmelpfennig, B.; Geist, A. *Inorg. Chem.* **2005**, *44*, 8418.
(24) Kolarik, Z.; Mullich, U.; Gassner, F. *Solvent Extr. Ion Exch.* **1999**, *17*, 23.
(25) Kolarik, Z.; Mullich, U.; Gassner, F. *Solvent Extr. Ion Exch.* **1999**, *17*, 1155.
(26) Hill, C.; Berthon, L.; Madic, C. Study of the stability of BTP extractants under radiolysis. *Proceedings of the International Conference on Nuclear Energy Systems for Future Generation and Global Sustainability* (GLOBAL 2005), Tsukuba, Japan, October 9−13, 2005.
(27) Hill, C.; Guillaneux, D.; Berthon, L.; Madic, C. *J. Nucl. Sci. Technol.* **2002**, No. Supplement 3, 309.
(28) Foreman, M. R. S.; Hudson, M. J.; Drew, M. G. B.; Hill, C.; Madic, C. *Dalton Trans.* **2006**, 1645.
(29) Geista, A.; Hillb, C.; Modoloc, G.; Std, M. R.; Foremand, J.; Weigla, M.; Gomppera, K.; Hudson, M. J. *Solvent Extr. Ion Exch.* **2006**, *24*, 463.
(30) Nilsson, M.; Andersson, S.; Drouet, F.; Ekberg, C.; Foreman, M.; Hudson, M.; Liljenzin, J. O.; Magnusson, D.; Skarnemark, G. *Solvent Extr. Ion Exch.* **2006**, *24*, 299.
(31) Retegan, T.; Ekberg, C.; Dubois, I.; Fermvik, A.; Skarnemark, G.; Wass, T. J. *Solvent Extr. Ion Exch.* **2007**, *25*, 417.
(32) Magnusson, D.; Christiansen, B.; Foreman, M. R. S.; Geist, A.; Glatz, J. P.; Malmbeck, R.; Modolo, G.; Serrano-Purroy, D.; Sorel, C. *Solvent Extr. Ion Exch.* **2009**, *27*, 97.
(33) Retegan, T.; Berthon, L.; Ekberg, C.; Fermvik, A.; Skarnemark, G.; Zorz, N. *Solvent Extr. Ion Exch.* **2009**, *27*, 663.
(34) Nilsson, M.; Ekberg, C.; Foreman, M.; Hudson, M.; Liljenzin, J. O.; Modolo, G.; Skarnemark, G. *Solvent Extr. Ion Exch.* **2006**, *24*, 823.
(35) Aneheim, E.; Ekberg, C.; Fermvik, A.; Foreman, M. R. S.; Retegan, T.; Skarnemark, G. *Solvent Extr. Ion Exch.* **2010**, *28*, 437.
(36) Drew, M. G. B.; Foreman, M. R. S. J.; Clement, H.; Hudson, M. J.; Madic, C. *Inorg. Chem. Commun.* **2005**, *8*, 239.
(37) Nilsson, M.; Andersson, S.; Drouet, F.; Ekberg, C.; Foreman, M.; Hudson, M.; Liljenzin, J.-O.; Magnusson, D.; Skarnemark, G. *Solvent Extr. Ion Exch.* **2006**, *24*, 299.
(38) Frisch, M. J.; Trucks, G. W.; Schlegel, H. B.; Scuseria, G. E.; Robb, M. A.; Cheeseman, J. R.; Montgomery, J. A., Jr.; Vreven, T.; Kudin, K. N.; Burant, J. C.; Millam, J. M.; Iyengar, S. S.; Tomasi, J.; Barone, V.; Mennucci, B.; Cossi, M.; Scalmani, G.; Rega, N.; Petersson, G. A.; Nakatsuji, H.; Hada, M.; Ehara, M.; Toyota, K.; Fukuda, R.; Hasegawa, J.; Ishida, M.; Nakajima, T.; Honda, Y.; Kitao, O.; Nakai, H.; Klene, M.; Li, X.; Knox, J. E.; Hratchian, H. P.; Cross, J. B.; Bakken, V.; Adamo, C.; Jaramillo, J.; Gomperts, R.; Stratmann, R. E.; Yazyev, O.; Austin, A. J.; Cammi, R.; Pomelli, C.; Ochterski, J. W.; Ayala, P. Y.; Morokuma, K.; Voth, G. A.; Salvador, P.; Dannenberg, J. J.; Zakrzewski, V. G.; Dapprich, S.; Daniels, A. D.; Strain, M. C.; Farkas, O.; Malick, D. K.; Rabuck, A. D.; Raghavachari, K.; Foresman, J. B.; Ortiz, J. V.; Cui, Q.; Baboul, A. G.; Clifford, S.; Cioslowski, J.; Stefanov, B. B.; Liu, G.; Liashenko, A.; Piskorz, P.; Komaromi, I.; Martin, R. L.; Fox, D. J.; Keith, T.; Al-Laham, M. A.; Peng, C. Y.; Nanayakkara, A.; Challacombe, M.; Gill, P. M. W.; Johnson, B.; Chen, W.; Wong, M. W.; Gonzalez, C.; Pople, J. A. *Gaussian 03*, revision C.01; Gaussian, Inc.: Wallingford, CT, 2004.
(39) Kuchle, W.; Dolg, M.; Stoll, H.; Preuss, H. *J. Chem. Phys.* **1994**, *100*, 7535.
(40) Cao, X.; Dolg, M. *J. Molec. Struct. (THEOCHEM)* **2004**, *673*, 203.
(41) Dolg, M.; Stoll, H.; Preuss, H. *J. Chem. Phys.* **1989**, *90*, 1730.
(42) Becke, A. D. *J. Chem. Phys.* **1993**, *98*, 5648.
(43) Reed, A. E.; Weinstock, R. B.; Weinhold, F. *J. Chem. Phys.* **1985**, *83*, 735.
(44) Kovacs, A.; Konings, R. J. M. *J. Phys. Chem. Ref. Data* **2004**, *33*, 377.
(45) Pantazis, D. A.; Neese, F. *J. Chem. Theory Comput.* **2009**, *5*, 2229.
(46) Shannon, R. D. *Acta Crystallogr.* **1976**, *A32*, 751.
(47) Becke, A. D.; Edgecombe, K. E. *J. Chem. Phys.* **1990**, *92*, 5397.
(48) Ciupka, J.; Cao-Dolg, X.; Wiebke, J.; Dolg, M. *Phys. Chem. Chem. Phys.* **2010**, *12*, 13215.
(49) Wiebke, J.; Moritz, A.; Cao, X.; Dolg, M. *Phys. Chem. Chem. Phys.* **2007**, *9*, 459.